HHS Public Access

Author manuscript

Biochemistry. Author manuscript; available in PMC 2017 July 26.

Published in final edited form as:

Biochemistry. 2016 July 26; 55(29): 4085–4091. doi:10.1021/acs.biochem.6b00479.

FtsZ Protofilament Curvature Is the Opposite of Tubulin Rings

Max Housman, **Sara L Milam**, **Desmond A Moore**, **Masaki Osawa**, and **Harold P. Erickson***

Department of Cell Biology, Duke University, Duke University Medical Center, Durham, North Carolina 27710, United States

Abstract

FtsZ protofilaments (pfs) form the bacterial cytokinetic Z ring. Previous work suggested that a conformational change from straight to curved pfs generated the constriction force. In the simplest model, the C-terminal membrane tether is on the outside of the curved pf, facing the membrane. Tubulin, a homologue of FtsZ, also forms pfs with a curved conformation. However, it is well-established that tubulin rings have the C terminus on the inside of the ring. Could FtsZ and tubulin rings have the opposite curvature? In this study, we explored the FtsZ curvature direction by fusing large protein tags to the FtsZ termini. Thin section electron microscopy showed that the C-terminal tag was on the outside, consistent with the bending pf model. This has interesting implications for the evolution of tubulin. Tubulin likely began with the curvature of FtsZ, but evolution managed to reverse direction to produce outward-curving rings, which are useful for pulling chromosomes.

Graphical abstract

*Corresponding Author: h.erickson@cellbio.duke.edu.

Author Contributions

S.E.M., M.O., and D.M. created constructs and did the preliminary characterization. M.H. did the EM and analysis, and D.M. did the light microscopy of Z rings with truncated linkers. M.H. and H.P.E. wrote the manuscript.

Notes

The authors declare no competing financial interest.

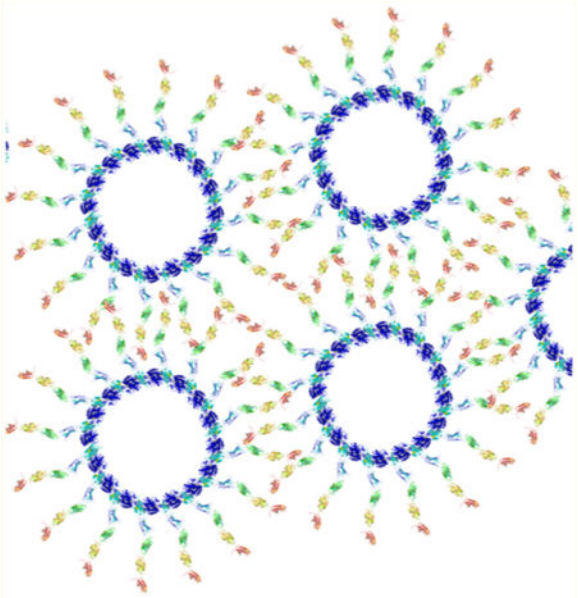

FtsZ is the primary cytoskeletal element in bacterial cytokinesis and is essential for cell division. FtsZ subunits assemble into protofilaments (pfs) that then assemble further to form the Z ring at the center of dividing bacteria. This Z ring acts as a scaffold for additional division proteins[1,2] and also exerts a constriction force on the plasma membrane to drive the invaginating septum.[3–5] Recent work suggesting that proteoglycan remodeling may provide the major constriction force[6] is addressed in Discussion.

FtsZ pfs have two extreme conformations, straight and highly curved.[7] We have proposed that the conformational change from straight to curved pfs generates a bending force on the membrane that leads to constriction.[7] The first experimental support for this model came from reconstitution of Z rings in liposomes by a purified FtsZ with a membrane targeting sequence attached (FtsZ-mts). Normally, FtsZ is tethered to the membrane by FtsA, which has an amphipathic helix that functions as a mts. Previous experiments in our lab[5] transferred the mts to the C terminus of FtsZ, producing FtsZ-mts, which could directly bind the membrane. When incorporated inside tubular liposomes, FtsZ-mts assembled into Z rings, and the Z rings generated force that constricted the liposomes. Both Z-ring assembly and constriction force were generated by FtsZ-mts alone and did not require any other protein. This was consistent with the bending hypothesis but did not prove it. Additional evidence came from switching the mts from the C terminus to the N terminus, which is on the opposite side of the FtsZ pf.[3] These switched pfs no longer assembled Z rings inside liposomes but assembled “inside-out” Z rings on the outside of liposomes. The inside-out Z rings also constricted the liposomes, squeezing from the outside. This supports the pf bending model, because the pf curvature is the same, and the preference for binding to the concave or convex lipid surface depends on the side of the pf to which the membrane tether was attached.

The eukaryotic cytoskeletal protein tubulin is a homologue of FtsZ.[8,9] Tubulin also assembles pfs, and they have straight and curved conformations.[10,11] The curved

conformation of tubulin is seen at the end of disassembling microtubules, where the pfs peel outward from the microtubule wall to form tight spirals and rings.[12] The tubulin rings can do mechanical work, because the bulge of tubulin rings provides a mechanism by which a disassembling microtubule can drag an attached chromosome.[13] The discovery of FtsZ minirings[7] suggested that that the curved conformation was conserved from FtsZ to eukaryotic α–β tubulin, with only a small change in diameter (24 nm for FtsZ and 42 nm for α–β tubulin).

However, the FtsZ bending-pf mechanism poses an apparent contradiction. In the simplest model, the tether needs to be on the outside of the curved pf, to face the concave membrane surface inside the bacterium or liposome. This places the C terminus of FtsZ, from which the tether exits, on the outside of the curved pf. In contrast, it is well established for tubulin rings that the C terminus, corresponding to the outside of a microtubule, is on the inside of the ring.[14–17] If our model is correct for FtsZ, the rings of tubulin and FtsZ would have to curve in opposite directions. To test this orientation, we prepared FtsZ with a protein tag fused to the N or C terminus and used electron microscopy (EM) to determine whether the tag was on the inside or outside of the curved pfs.

EXPERIMENTAL PROCEDURES

Protein Purification and Assembly

FtsZ constructs were expressed in *Escherichia coli* and purified by ammonium sulfate precipitation and Resource Q anion exchange column; 20% saturated ammonium sulfate was used to precipitate the majority of bacterial proteins. The ammonium sulfate concentration was increased to 30% saturation to precipitate the FtsZ. The protein was then dialyzed into Ltk50 buffer [50 mM Tris-HCl, 50 mM KCl, 1 mM EDTA, and 10% glycerol (pH 7.9)] and purified on a Resource Q anion exchange column. Peak fractions were dialyzed into HMK100 buffer [50 mM HEPES, 100 mM KAc, and 5 mM MgAc (pH 7.6)], with 10% glycerol added for storage at −80 °C. Concentration was measured by tryptophan fluorescence where available or BCA assay using a BSA standard and multiplying by 0.75 to correct for the weakened color of FtsZ.[18] The purification was essentially the same for wild-type FtsZ (wtFtsZ), FN-FtsZ and FtsZ-FN [FtsZ with fibronectin (FN) fragment FN7–10 fused to the N and C termini, respectively], and FtsZ-mVenus (with the YFP variant mVenus fused to the C terminus).

All reactions were conducted in HMK100 buffer, with 1 mg/mL protein and 2 mM nucleotide. Filaments were assembled by adding GTP and incubating the mixtures for 10 min at room temperature. Tubes were assembled by adding GDP, waiting 1 min, adding DEAE-dextran, and incubating samples for 10 min at room temperature. The amount of DEAE-dextran added was 0.25 mg/mL for wtFtsZ, 0.5 mg/mL for FtsZ-mVenus, and 1.5 mg/mL for FtsZ-FN.

Assembly of Z Rings with Truncated Linkers

To determine whether FtsZ with truncated linkers can still assemble Z rings, we used the construct FtsZ-G55-mVenus-Q56–366-mts, where the YFP variant mVenus is inserted in a

loop between FtsZ amino acids G55–Q56 (D. Moore et al., manuscript submitted for publication), and the amphipathic helix from MinD is attached at amino acid 366, replacing the conserved FtsA-binding peptide.[5] This construct has the full length linker. We prepared additional constructs 341-mts, 321-mts, and 316-mts, where the mts was attached at the indicated amino acid. In 316-mts, the mts is attached to the last amino acid of the globular domain, completely deleting the linker. These constructs were expressed from plasmid pJSB2 in *E. coli* strain JKD7-pKD3, in which wtFtsZ can be depleted by increasing the temperature to 42 °C.[19] JKD7 cells were diluted 1:100 in LB via an overnight culture at 30 °C under repression conditions and then grown at 42 °C for 5 h. Samples were viewed via fluorescence microscopy on a Zeiss Axiophot microscope with a plan-Neofluar 100× NA 1.3 oil immersion lens. Filter cubes optimized for YFP were used for fluorescence microscopy. Images were acquired with a Coolsnap HQ CCD camera (Roper Scientific) and processed with Adobe Photoshop.

Electron Microscopy and Staining

Negative stain samples were prepared by adding 10 μL of assembled protein to a carbon-coated grid. The sample was removed and the grid stained with 5 drops of 2% uranyl acetate. Samples for embedding and sectioning were prepared as described previously.[20] Assembled tubes were fixed in 1% glutaraldehyde and centrifuged, and pellets were further fixed in 3% glutaraldehyde and 0.2% tannic acid. They were then stained with 1% osmium tetroxide for 30–60 min, followed by block staining with 2% uranyl acetate. The samples were then dehydrated and embedded in Araldite resin. Silver and gray sections (50–70 nm) were collected for observation by EM. Electron microscopy was performed using a Philips 420 microscope, and images were collected at 49000× magnification unless otherwise stated.

Image and Statistical Analysis

Images were analyzed and measured in FIJI (Is Just ImageJ). Statistical analysis was performed in Microsoft Excel. Analysis of variance (ANOVA) tests were run on all sets with a p value result of 0 (below the calculation threshold of Excel). Brightness and contrast were adjusted in Photoshop for optimal presentation of images.

RESULTS

FtsZ Tubes as the Model for the Highly Curved Conformation

The highly curved conformation of *E. coli* FtsZ was first seen for polymers assembled in vitro and adsorbed to cationic lipid monolayers, where it formed “minirings” 24 nm in diameter.[7] However, minirings do not assemble in solution; the closed circular form is apparently imposed by adsorption to the flat lipid monolayer. An alternative form of the highly curved conformation is the FtsZ tube, which is assembled by FtsZ with the addition of GDP and DEAE-dextran.[20] The tube is formed by three or four pfs of FtsZ spiraling in a helical assembly. The tube has the same 24 nm diameter as the miniring, but the pfs also have a pitch of 22 nm. The tubes are large, stable, and much easier to manipulate and image than the minirings. For these reasons, we performed our experiments with DEAE-dextran tubes instead of minirings. Negative stain EM images of tubes are shown in Figure 1.

Protein Fusions To Tag the C and N Termini of FtsZ

The C terminus of FtsZ comprises a 50-amino acid flexible linker and a conserved 17-amino acid peptide that binds to FtsA and hence the membrane. For the C-terminal fusion, we removed this tether and fused the protein tag after amino acid 316, the last amino acid in the globular domain. The N terminus of FtsZ is a nine-amino acid flexible peptide on the opposite side of the pf. For the N-terminal fusion, we fused the tag in front of amino acid 1.

The first protein tag is FN7–10, a segment of fibronectin (FN) comprising four FNIII domains. FN7–10 is 40 kDa, a mass that is approximately the same as that of FtsZ, but forms an extended rod that is 14 nm long and 2.5 mm × 3 nm wide.[21] Figure 2A shows a model of the structure of FtsZ-FN. If the bending pf model is correct, in the N-terminal fusion (FN-FtsZ), the FN7–10 rod should face the inside of the tube. However, this construct should be incapable of making tubes, because the FN rods would not fit in the interior (Figure 2B). FtsZ-FN, with the FN on the C terminus, should assemble tubes with the FN rods extending outward (Figure 2C).

The second tag is the yellow fluorescent protein mVenus. This is a smaller protein, 27 kDa, and globular, but still large enough that it should sterically inhibit tube assembly if it is projecting to the inside. For FtsZ-mVenus, the C-terminal tether was left intact and mVenus was fused after amino acid 383.

Assembly of FtsZ Fusion Constructs

We first tested each of the fusion constructs for assembly without DEAE-dextran. All of the constructs (FN-FtsZ, FtsZ-FN, mVenus-FtsZ, and FtsZ-mVenus) were capable of forming pfs in HMK100 buffer with GTP, as imaged via negative stain EM. We had hoped that the fusions might provide a visible distinction, namely that the pfs would appear thicker or fuzzy, but there was no visible difference of pfs with or without an FN or mVenus tag.

The FN-FtsZ and mVenus-FtsZ constructs (N-terminal fusions) were unable to form tubes. These results fit with our hypothesis that the N terminus of FtsZ faces the interior of the tube. There should not be sufficient room in the interior of the tube to fit the FN domains or mVenus, posing a steric block for tube formation by the N-terminal fusions.

The C-terminal fusions, FtsZ-FN and FtsZ-mVenus, were both capable of forming tubes under these conditions. However, when observed by negative stain EM, the tubes of different constructs could not be distinguished (Figure 1B,C). They all had a uniform width of ~25 nm. We conclude that uranyl acetate negative stain was not sensitive enough to visualize the FN or mVenus extensions to the FtsZ.

We therefore transitioned to embedding and thin sectioning, with alternative positive staining, where the FtsZ shows up as a dark ring of stain. The embedded tubes were in random orientations. The most informative orientation was the cross section, and these were selected for measurement. The tubes appeared to cluster into parallel arrays, perhaps a result of the fixation and centrifugation process. This allowed us to measure the center to center distance of neighboring tubes. This measurement is more precise than the outside diameter

of a tube, especially for the FN and mVenus constructs, where it can be difficult to distinguish boundaries between neighboring tubes.

In addition to the different measurements of the tubes discussed below, the different constructs could be distinguished by their appearance in a positive stain thin section (Figure 3). The FtsZ-FN tubes have a dark ring of stain that has a width and a diameter that are the same as those of the wild-type construct and is identified as the FtsZ. However, they are surrounded by a large pale halo. This is presumably the FN7–10 tag, which apparently does not absorb the stain as well as the FtsZ. The mVenus construct, in contrast, produces a uniform dark stain that cannot be distinguished from the FtsZ. The FtsZ-mVenus tubes also have a much more regular packing, producing large fields of regular, hexagonal lattices.

Several measurements support the conclusion that the C-terminal FN and mVenus tags project on the outside of the tubes (Figure 4). The width of the lumen of the wild-type tubes was ~9.9 nm. The lumens of the FtsZ-FN and FtsZ-mVenus tubes were ~9.2 and ~9.4 nm, respectively. While this is a slight decrease in lumen width, the difference is much too small to suggest that the protein addition is on the interior of the tube.

The most informative measure of the C-terminal tags was the center to center spacing of the tubes in cross-section clusters. This was 21.4 nm for wtFtsZ, 30.7 nm for FtsZ-FN, and 28.6 nm for FtsZ-mVenus. The FN domains are 14 nm long when they are fully extended, which is longer than the ~9 nm increase in tube separation. This suggests that the FN extensions from adjacent tubes interdigitate, which is compatible with the thin dimensions of the FN7–10 rod (2.5 nm × 3.5 nm × 14 nm) (Figure 2A). However, the ~9 nm increased separation is less than the 14 nm length of the FN rod, which suggests that the FN rods are not extended perpendicular to the tube axis but are bent at the flexible point of attachment to FtsZ amino acid 316. The 7 nm increased spacing for the FtsZ-mVenus tubes is compatible with a fairly close packing of mVenus tags, which is a 3 nm × 3 nm × 4.5 nm barrel.

Z Rings Assembled in *E. coli* from FtsZ-YFP-mts with Shortened and Deleted Linkers

While the simplest model of the pf bending mechanism places the C terminus and the linker on the outside of the curved pf, directly facing the membrane (Figure 5A1), an alternative model has been proposed to explain the curvature seen in a crystal structure of FtsZ from *Mycobacterium tuberculosis*.[22] In this model, the C terminus is on the inside of the curved pf and the linker, a disordered peptide of 50 amino acids, loops around the pf to emerge on the outside and eventually attach to the membrane (Figure 5A2). This might be possible with the natural linker of 50 amino acids, but shortening the linker would compromise the assembly of Z rings. We tested this using a construct FtsZ-YFP-mts, in which mts is an amphipathic helix that attaches FtsZ directly to the membrane. We previously showed that FtsZ-YFP-mts assembled extensive Z rings and spirals when expressed in *E. coli* strain JKD7-pKD3, in which wtFtsZ can be depleted by increasing the temperature to 42 °C.[5] For this study, we prepared FtsZ-YFP-mts with the linker shortened or deleted entirely. Figure 5B shows that all of these constructs assembled extensive Z rings and helices when expressed in JKD7-pKD3 depleted of wtFtsZ, including the construct mts-316, from which the linker is deleted completely. This is only possible with model Figure 5A1, adding further support to our interpretation of curvature.

DISCUSSION

The C-Terminal Membrane Tether Is on the Outside of Curved FtsZ pfs

We previously proposed that the Z-ring constriction force is generated by FtsZ pfs switching from a straight to a curved conformation. The simplest model required that the C-terminal membrane tether exit from the outside of the curved pf.[3,23,24] This is the opposite of the curvature of tubulin rings, which have the C terminus on the inside, presenting an apparent contradiction. In the study presented here, we demonstrate that a large protein tag fused to the C terminus of FtsZ is indeed on the outside of the curved pfs, as predicted by our model.

A recent crystal structure of FtsZ from *M. tuberculosis* showed antiparallel pf pairs in a tight spiral, with the C terminus facing inward.[22] A more complex model of pf bending was presented, in which the flexible linker originated on the inside of the curved pf and looped around the pf to exit on the outside of the curve and toward the membrane (Figure 5A2). However, we show here that FtsZ-YFP-mts can assemble Z rings and helices in *E. coli* cells with the linker shortened or even deleted (Figure 5B). In the case of FtsZ-YFP-mts-316, the amphipathic helix is attached directly to the C terminus of the globular FtsZ, which would place it in direct contact with the membrane. In a separate study, *Caulobacter crescentus* FtsZ could function for cell division with its linker reduced to 14 amino acids.[25] This also argues against the model in Figure 5A2.

The pf curvature in the *M. tuberculosis* crystals is the opposite of what we show for *E. coli* pfs, and it is not yet clear if it is physiologically important. The helix in the crystal structure was much more highly curved, with an outside diameter of 12–13 nm, versus the 21–24 nm diameter of the tubes. Also, the surface area buried in the interface of the crystal helical pfs was 1040 Å^2, less than half that in the straight pf of *Staphylococcus aureus* FtsZ (2360 Å^2[26]). Modeling studies have predicted that FtsZ and tubulin pfs can bend in both directions.[27–30] The helix in the *M. tuberculosis* crystals suggests that the opposite curvature can actually be realized for FtsZ. However, we conclude that this curvature is not the one generating a constriction force.

In addition to the highly curved miniring/tube conformation, FtsZ pfs have an intermediate curved conformation, with a diameter of ~200 nm. This curved conformation gives rise to toroids and helical bundles under various crowding conditions,[31] and it may be the major source of constriction force.[4] We have not been able to image protein tags on the intermediate curved conformation, so the direction of curvature has also not been determined. We can only suggest that the intermediate curved conformation is indeed intermediate to the highly curved pf and is bending in the same direction. The Z rings reconstituted with FtsZ-YFP-mts-316 provide evidence that whatever curved conformation is relevant in vivo, its C terminus faces the membrane.

Is the Constriction Force Generated by FtsZ or by Peptidoglycan Remodeling?

The “Z-centric hypothesis”, that bending pfs generate the constriction force, has been questioned by Coltharp et al.[6] They examined how mutations in either FtsZ or proteoglycan synthesis affected the timing of constriction onset and the rate of septum invagination. They found that the time of constriction onset and the rate of septum invagination were not

affected by the FtsZ84 mutant, which has reduced GTPase and exchange dynamics. In contrast, alterations in proteoglycan synthesis affected both constriction onset and the rate of invagination. They concluded that “septum closure is likely driven by septum synthesis rather than Z-ring contraction.”

The idea that peptidoglycan remodeling might provide the primary driving force for septation has a long history. In the extreme scenario, the ring of FtsZ is proposed to serve primarily as a docking site for the remodeling enzymes, and the constriction force is generated entirely by the inward remodeling of the peptidoglycan. This was largely discounted when FtsZ was discovered in mycoplasma and archaea, which have no peptidoglycan cell wall.[32–34] Because FtsZ, but none of the other Fts proteins, is found in mycoplasma and archaea, FtsZ was boosted as the prime candidate for generating the constriction.

The observations of Coltharp et al.[6] are actually consistent with our model, in which FtsZ is the primary source of constriction force. We suggest specifically that FtsZ84, although having reduced GTPase and dynamics, can still generate a constriction force that is sufficient to drive septum invagination. However, regardless of the magnitude of the force generated by FtsZ, constriction cannot begin until peptidoglycan remodeling permits the cell wall to follow. Likewise, the rate of septum invagination is probably limited, not by the force generated by FtsZ but by the rate at which remodeling permits the peptidoglycan wall to follow the inner membrane. Peptidoglycan remodeling is a chemical process likely independent of the force generated on the other side of the membrane. In the scenario we propose, septum invagination is driven by the constriction force of FtsZ, but its rate is limited by peptidoglycan remodeling, which allows the wall to passively follow.

In bacteria with a peptidoglycan wall, peptidoglycan remodeling is still a candidate for contributing to the constriction force,[6,35] perhaps especially in the later stage. However, there is no compelling evidence that proteoglycan remodeling actually does generate force. In contrast, in vitro reconstitution has shown that FtsZ alone can constrict even thick-walled multilamellar lipid tubes.[3–5]

Evolution of the Opposite Curvature in Tubulin pfs

A second important conclusion from our study is that pfs in tubulin rings are apparently bending in the opposite direction to FtsZ pfs. The curvature of microtubule pfs seems to be essential for two microtubule functions. First, the tuft of curved pfs at the end of a disassembling microtubule provides a steric wedge that permits the disassembling microtubule to drag cargo like chromosomes.[13] Second, the strained bonds introduced by curvature of the terminal subunits may be key to the important mechanism of microtubule dynamic instability.[36,37] We can speculate about how tubulin pfs evolved a curvature that was the opposite of that of FtsZ. We would propose that the precursor of tubulin in early eukaryotes had the same direction of curvature as FtsZ. However, it was the straight conformation that was important in assembling sheets of pfs, which eventually formed the microtubule wall. These pfs would have the ability to curve when they separated from neighboring pfs at the ends of the microtubules. pfs with the FtsZ curvature would bend toward the inside of the microtubule, where they might interfere with each other. This

curvature may have been lost in the early stages of microtubule evolution. Subsequent evolution generated an outward curvature, which became advantageous for the mechanical work of dragging chromosomes.

Acknowledgments

We thank the lab of Dr. Michael Reedy for EM and thin sectioning support.

Funding

The work was supported by National Institutes of Health Grant GM66014.

ABBREVIATIONS

pf
protofilament

FN
fibronectin

FN-FtsZ and FtsZ-FN
FtsZ with fibronectin fragment FN7–10 fused to the N and C termini, respectively

mVenus-FtsZ and FtsZ-mVenus
FtsZ with mVenus fused to the N and C termini, respectively

wtFtsZ
wild-type FtsZ

mts
membrane targeting sequence

References

1. Rowlett VW, Margolin W. The bacterial divisome: ready for its close-up. Philos Trans R Soc, B. 2015; 370:20150028.
2. Lutkenhaus J, Pichoff S, Du S. Bacterial cytokinesis: From Z ring to divisome. Cytoskeleton. 2012; 69:778–790. [PubMed: 22888013]
3. Osawa M, Erickson HP. Inside-out Z rings-constriction with and without GTP hydrolysis. Mol Microbiol. 2011; 81:571–579. [PubMed: 21631604]
4. Erickson HP, Anderson DE, Osawa M. FtsZ in Bacterial Cytokinesis: Cytoskeleton and Force Generator All in One. Microbiol Mol Biol Rev. 2010; 74:504–528. [PubMed: 21119015]
5. Osawa M, Anderson DE, Erickson HP. Reconstitution of contractile FtsZ. rings in liposomes. Science. 2008; 320:792–794. [PubMed: 18420899]
6. Coltharp C, Buss J, Plumer TM, Xiao J. Defining the rate-limiting processes of bacterial cytokinesis. Proc Natl Acad Sci U S A. 2016; 113:E1044. [PubMed: 26831086]
7. Erickson HP, Taylor DW, Taylor KA, Bramhill D. Bacterial cell division protein FtsZ assembles into protofilament sheets and minirings, structural homologs of tubulin polymers. Proc Natl Acad Sci U S A. 1996; 93:519–523. [PubMed: 8552673]
8. Nogales E, Wolf SG, Downing KH. Structure of the $\alpha\beta$ tubulin dimer by electron crystallography. Nature. 1998; 391:199–203. [PubMed: 9428769]

9. Löwe J, Amos LA. Crystal structure of the bacterial cell-division protein FtsZ. Nature. 1998; 391:203–206. [PubMed: 9428770]
10. Kirschner MW, Williams RC, Weingarten M, Gerhart JC. Microtubules from mammalian brain: some properties of their depolymerization products and a proposed mechanism of assembly and disassembly. Proc Natl Acad Sci U S A. 1974; 71:1159–1163. [PubMed: 4524627]
11. Erickson HP. Assembly of microtubules from preformed, ring-shaped protofilaments and 6-S tubulin. J Supramol Struct. 1974; 2:393–411. [PubMed: 4474573]
12. Mandelkow EM, Mandelkow E, Milligan RA. Microtubule dynamics and microtubule caps: a time-resolved cryoelectron microscopy study. J Cell Biol. 1991; 114:977–991. [PubMed: 1874792]
13. McIntosh JR, Volkov V, Ataullakhanov FI, Grishchuk EL. Tubulin depolymerization may be an ancient biological motor. J Cell Sci. 2010; 123:3425–3434. [PubMed: 20930138]
14. Nawrotek A, Knossow M, Gigant B. The determinants that govern microtubule assembly from the atomic structure of GTP-tubulin. J Mol Biol. 2011; 412:35–42. [PubMed: 21787788]
15. Tan D, Rice WJ, Sosa H. Structure of the kinesin13-microtubule ring complex. Structure. 2008; 16:1732–1739. [PubMed: 19000825]
16. Moores CA, Milligan RA. Visualisation of a kinesin-13 motor on microtubule end mimics. J Mol Biol. 2008; 377:647–654. [PubMed: 18294653]
17. Wang HW, Nogales E. Nucleotide-dependent bending flexibility of tubulin regulates microtubule assembly. Nature. 2005; 435:911–915. [PubMed: 15959508]
18. Lu C, Stricker J, Erickson HP. FtsZ from Escherichia coli, Azotobacter vinelandii, and Thermotoga maritima-quantitation, GTP hydrolysis, and assembly. Cell Motil Cytoskeleton. 1998; 40:71–86. [PubMed: 9605973]
19. Osawa M, Erickson HP. FtsZ from divergent foreign bacteria can function for cell division in *Escherichia coli*. J Bacteriol. 2006; 188:7132–7140. [PubMed: 17015652]
20. Lu C, Reedy M, Erickson HP. Straight and curved conformations of FtsZ are regulated by GTP hydrolysis. J Bacteriol. 2000; 182:164–170. [PubMed: 10613876]
21. Leahy DJ, Hendrickson WA, Aukhil I, Erickson HP. Structure of a fibronectin type III domain from tenascin phased by MAD analysis of the selenomethionyl protein. Science. 1992; 258:987–991. [PubMed: 1279805]
22. Li Y, Hsin J, Zhao L, Cheng Y, Shang W, Huang KC, Wang HW, Ye S. FtsZ protofilaments use a hinge-opening mechanism for constrictive force generation. Science. 2013; 341:392–395. [PubMed: 23888039]
23. Osawa M, Anderson DE, Erickson HP. Curved FtsZ protofilaments generate bending forces on liposome membranes. EMBO J. 2009; 28:3476–3484. [PubMed: 19779463]
24. Arumugam S, Chwastek G, Fischer-Friedrich E, Ehrig C, Monch I, Schwille P. Surface topology engineering of membranes for the mechanical investigation of the tubulin homologue FtsZ. Angew Chem, Int Ed. 2012; 51:11858–11862.
25. Sundararajan K, Miguel A, Desmarais SM, Meier EL, Casey Huang K, Goley ED. The bacterial tubulin FtsZ requires its intrinsically disordered linker to direct robust cell wall construction. Nat Commun. 2015; 6:7281. [PubMed: 26099469]
26. Matsui T, Yamane J, Mogi N, Yamaguchi H, Takemoto H, Yao M, Tanaka I. Structural reorganization of the bacterial cell-division protein FtsZ from Staphylococcus aureus. Acta Crystallogr, Sect D: Biol Crystallogr. 2012; 68:1175–1188. [PubMed: 22948918]
27. Ramirez-Aportela E, Lopez-Blanco JR, Andreu JM, Chacon P. Understanding nucleotide-regulated FtsZ filament dynamics and the monomer assembly switch with large-scale atomistic simulations. Biophys J. 2014; 107:2164–2176. [PubMed: 25418101]
28. Theisen KE, Zhmurov A, Newberry ME, Barsegov V, Dima RI. Multiscale modeling of the nanomechanics of microtubule protofilaments. J Phys Chem B. 2012; 116:8545–8555. [PubMed: 22509945]
29. Hsin J, Gopinathan A, Huang KC. Nucleotide-dependent conformations of FtsZ dimers and force generation observed through molecular dynamics simulations. Proc Natl Acad Sci U S A. 2012; 109:9432–9437. [PubMed: 22647609]
30. Grafmuller A, Voth GA. Intrinsic bending of microtubule protofilaments. Structure. 2011; 19:409–417. [PubMed: 21397191]

31. Popp D, Iwasa M, Narita A, Erickson HP, Maeda Y. FtsZ condensates: An in vitro electron microscopy study. Biopolymers. 2009; 91:340–350. [PubMed: 19137575]
32. Wang X, Lutkenhaus J. Characterization of FtsZ from *Mycoplasma pulmonis*, an organism lacking a cell wall. J Bacteriol. 1996; 178:2314–2319. [PubMed: 8636032]
33. Wang X, Lutkenhaus J. FtsZ ring: the eubacterial division apparatus conserved in archaebacteria. Mol Microbiol. 1996; 21:313–319. [PubMed: 8858586]
34. Margolin W, Wang R, Kumar M. Isolation of an ftsZ homolog from the archaebacterium *Halobacterium salinarium*: Implications for the evolution of FtsZ and tubulin. J Bacteriol. 1996; 178:1320–1327. [PubMed: 8631708]
35. Meier EL, Goley ED. Form and function of the bacterial cytokinetic ring. Curr Opin Cell Biol. 2014; 26:19–27. [PubMed: 24529242]
36. Zakharov P, Gudimchuk N, Voevodin V, Tikhonravov A, Ataullakhanov FI, Grishchuk EL. Molecular and Mechanical Causes of Microtubule Catastrophe and Aging. Biophys J. 2015; 109:2574–2591. [PubMed: 26682815]
37. VanBuren V, Odde DJ, Cassimeris L. Estimates of lateral and longitudinal bond energies within the microtubule lattice. Proc Natl Acad Sci U S A. 2002; 99:6035–6040. [PubMed: 11983898]

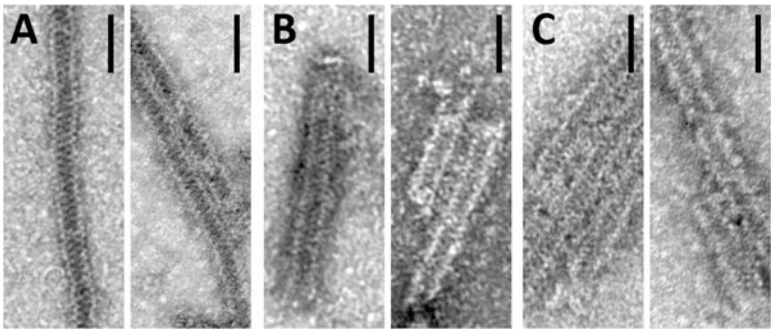

Figure 1.

Negative stain electron micrographs of tubes of FtsZ assembled with GDP and DEAE-dextran. Tubes with (B) FN7–10 or (C) mVenus fusions have the same measurements as (A) native FtsZ, and the peptide additions are not visible. The scale bar is 50 nm.

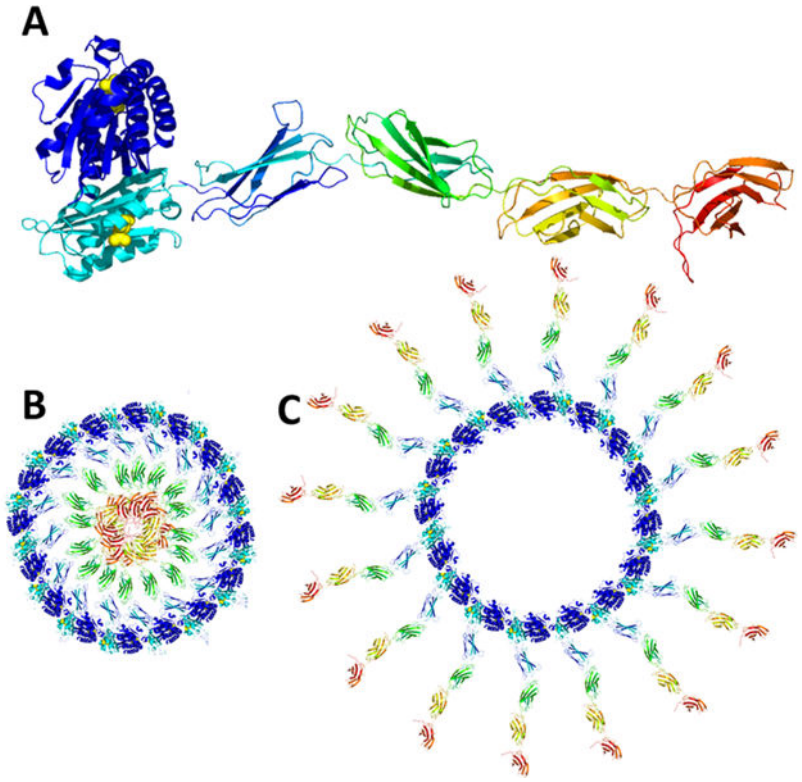

Figure 2.

Model of FtsZ with FN7–10 domains attached to the C terminus. (A) FtsZ is the blue globular domain on the left. The four smaller teal through red domains are the fibronectin type III domains. (B) Model of the tube if the C terminus is facing the interior of the tube. Note that there is not enough space to fit all of the FN. This tube should not be able to form. (C) Model of the tube if the N terminus is facing the exterior. Note the spread out FN domains that are not conflicting with each other in any way.

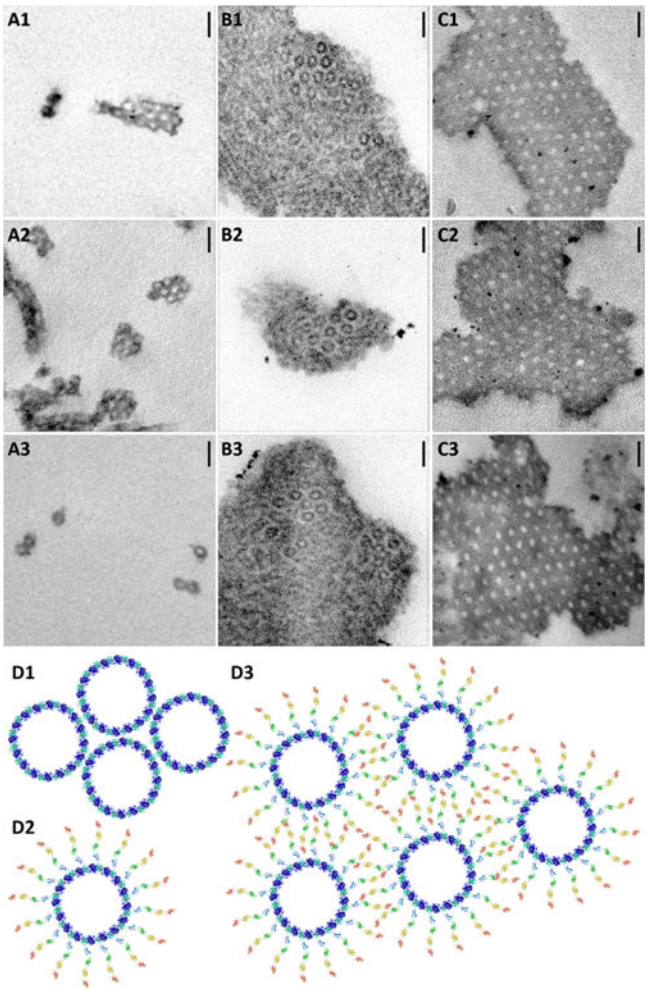

Figure 3.

Thin (50 nm) sections of FtsZ tubes. The scale bar is 50 nm. Column A shows wtFtsZ tubes. Note the distinct ring of dark stain around the open lumen. Tubes have limited clustering and are closely packed. Column B shows FtsZ-FN tubes. Note the increased level of clustering in random orientations. The tubes cluster in a parallel manner only in small patches. The same dark ring of FtsZ can be seen as in the wtFtsZ. Note the large white halo surrounding the FtsZ rings, and the greatly increased separation. This is attributed to the FN, which does not stain as darkly as the FtsZ. Column C shows FtsZ-mVenus tubes. Note the large patches of clustered, parallel tubes. The protein staining is uniform, with mVenus staining not differentiated from that of the FtsZ. Section D depicts a model showing interdigitation of FN domains in clustered tubes. (D1) Closely packed clustering of wtFtsZ tubes. (D2) Single FtsZ-FN tube. Note the large, uniform halo of FN. (D3) Clustering of FtsZ-FN tubes. Note that the width of the halo of a single tube is the same as the width of the halo between neighboring tubes in the thin section. This suggests interdigitation, as is seen in the model.

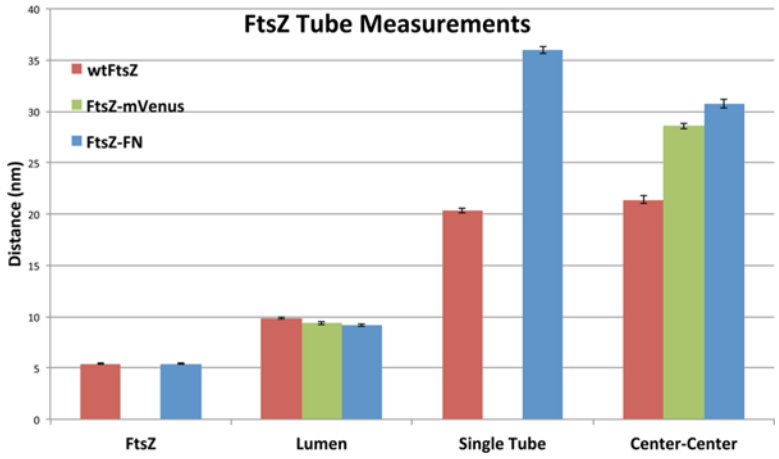

Figure 4.

Graph of FtsZ tube measurements. “FtsZ” indicates the width of the FtsZ wall (not available for FtsZ-mVenus). “Lumen” is the inside diameter of the tubes. “Single Tube” is the diameter, including the halo for FtsZ-FN. “Center–Center” is the spacing of tubes measured from the center of the lumen. Note that the single-tube width of the FtsZ-FN construct is greater than the center–center width of neighboring tubes. This is due to interdigitation of the FN domains. For statistical analysis, ANOVA was performed and error bars are the standard error of the mean.

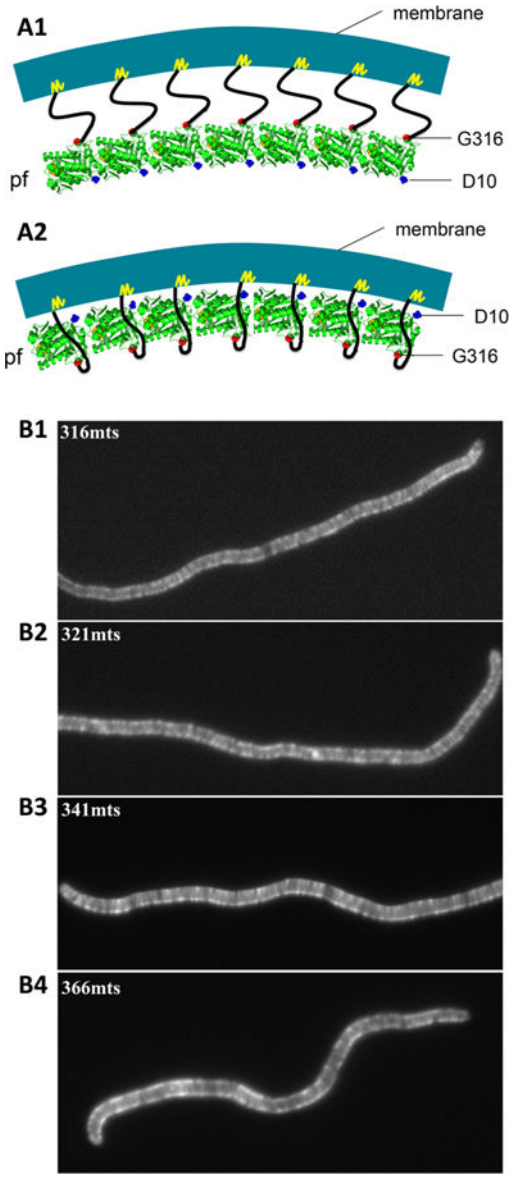

Figure 5.

(A) Models showing two possibilities for the curvature of the FtsZ pf relative to the membrane. The FtsZ globular domain is colored green, the 55-amino acid linker black, and the mts yellow. (A1) The C terminus faces the outside of the curved pf, as determined in this study. The C-terminal tail could be shortened or eliminated, and the mts could still attach to the membrane. (A2) The C terminus faces the inside of the curved pf, for tubulin and found in a crystal structure of *M. tuberculosis* FtsZ.[22] In this case, the C-terminal tail would have to wrap completely around the FtsZ to attach to the membrane, and the linker could not be eliminated. (B) FtsZ-YFP-mts can form Z rings in bacteria with truncated linkers. (B1) The mts is directly attached to the globular domain at amino acid 316. These cells still form Z rings, excluding model A2. (B2–B4) Various truncations of the FtsZ linker are still able to attach to the membrane to form Z rings. These images further support the model in panel

A1. The cells form numerous Z rings all along the length of the bacterium, appearing as fluorescent bands.